

Sound wave propagation in strongly elongated fermion clouds at finite collisionality

P Capuzzi, P Vignolo, F Federici and M P Tosi

NEST-INFM-CNR and Classe di Scienze, Scuola Normale Superiore, I-56126 Pisa, Italy

E-mail: capuzzi@sns.it, vignolo@sns.it, fr.federici@sns.it, tosim@sns.it

Abstract. We evaluate the transition from zero-sound to first-sound behaviour with increasing collisionality in the propagation of density waves through an ultracold gaseous mixture of fermionic atoms confined in the normal state inside a cigar-shaped harmonic trap. We study for this purpose the evolution of the one-body distribution functions associated with a density perturbation generated in the central region of the cloud, as obtained by solving numerically the Vlasov-Landau equations. We examine a variety of trap anisotropies and of repulsive or attractive interaction strengths between the components of the mixture, and the speed of propagation of the density disturbance is found to decrease in both cases as the magnitude of the coupling strength is increased. The results are compared with the values of the speed of zero sound and of first sound, as obtained analytically from the limit of vanishing collisionality and from linearized hydrodynamics. The main effects of the quasi-one-dimensional confinement are the stabilization of zero-sound excitations in the attractive regime before collapse and the lowering of the hydrodynamic sound velocity by a factor $\sqrt{3/5}$ relative to three-dimensional behaviour.

Submitted to: *J. Phys. B: At. Mol. Phys.*

PACS numbers: 03.75.Ss, 05.30.Fk, 02.70.Ns

1. Introduction

Several experiments on mixed Fermi gases consisting of two components with different pseudospins have probed their collisional properties both in the normal [1] and in the superfluid state [2, 3]. In the experiments performed by the JILA group, the collisionality of a ^{40}K mixture in the normal state was tuned by varying either the atomic density [1, 4] or the off-resonant value of the scattering length [5, 6]. Gensemer and Jin [1] examined the frequency and damping of the dipolar modes of the mixture as functions of its collisionality, showing that, while in the collisionless limit the two components oscillate independently with vanishing damping, on increasing the strength of the mutual repulsive interactions the damping first increases and then decreases until in the hydrodynamic limit the two components oscillate together at the same frequency without damping. The same behaviour has been obtained from numerical simulations [7, 8]. The absence of damping in the two opposite limits signals the existence of long-lived collective sound-wave excitations in suitable system geometries, the so-called zero sound in the collisionless limit and the hydrodynamic first sound in the strongly collisional regime.

More recently attention has focused on sound-wave propagation in a Fermi gas with attractive interactions ranging in strength from the BCS to the BEC regime [9–12]. Below the critical temperature for the transition to a superfluid state, the presence of both normal and superfluid components leads to two acoustic modes corresponding to the propagation of density waves and thermal waves [9, 13]. These modes contain information on the equation of state of the gas and on the geometry of the system [11] and impose constraints on the appropriate theoretical models to describe the BCS-BEC crossover [10]. Above the critical temperature the speed of propagation of a density perturbation still gives information about the shape of the equilibrium density profiles and about the collisionality of the gas relative to the frequency of the perturbation.

The behaviour that we have recalled above for the attenuation of sound waves as a function of collisionality was predicted in the early work of Landau on normal liquid ^3He [14]. In the experiments of Abel *et al.* [15] on this liquid, the collisionality was explored by tuning the frequency of an acoustic disturbance. The experiment demonstrated that the transition from collisional to collisionless dynamics is signalled by a drastic change in the frequency dependence of the attenuation and showed that the ratio of the speeds of zero and first sound is very much smaller than the value $\sqrt{3}$ expected for a homogeneous fluid at weak coupling. In a dilute Fermi gas one should expect that the interactions introduce instead only slight modifications to the bare sound velocities in the ideal Fermi gas.

The main purpose of the present work is to provide direct theoretical evidence for the transition from zero to first sound in a normal Fermi gas by evaluating the propagation of density waves in a two-component mixture confined inside an elongated cigar-shaped harmonic trap. We have in mind an experiment in which the collisionality could be varied by tuning the scattering length a as can be realized by exploiting

Feshbach resonances [5] and the density perturbation could be generated by a laser beam focused at the centre of the trap [16]. We perform numerical simulations of the dynamics of the gas, in which collisions are taken into account by solving the Vlasov-Landau equations (VLE) for the one-body distribution functions of the two fermionic components. We observe that on increasing the scattering cross-section the velocity of propagation of the density distortions, which is given by the Fermi velocity v_F in the collisionless limit, diminishes for both attractive and repulsive coupling. If the mean-field corrections are negligible, the hydrodynamic limit for the confined gas in the elongated trap yields a propagation velocity $v_F/\sqrt{5}$ instead of $v_F/\sqrt{3}$ as appropriate to a homogeneous gas. Most remarkably, the zero-sound excitation is found to be stable even at weak attractive couplings, before the attractions drive the gas to collapse.

The paper is organized as follows. In Sec. 2 we introduce the fermion mixture under study and discuss the dynamical regimes that can be realized in a dilute gaseous state, a detailed analytic calculation for zero sound in a cylindrical trap being reported in an Appendix. In Sec. 3 we present our treatment of a mixture with finite collisionality and discuss our numerical results for the velocity of propagation of density waves. Finally, Sec. 4 offers a summary and the main conclusions of the work.

2. The model system

We consider a mixture of two species of fermionic atoms of mass m confined in a harmonic trap of the form

$$V_{\text{ext}}(\mathbf{r}) = \frac{1}{2} m \omega_{\perp}^2 (r_{\perp}^2 + \lambda^2 z^2), \quad (1)$$

where $\lambda = \omega_z/\omega_{\perp}$ is the anisotropy parameter. The atoms of each species are spin-polarized and the gas is highly dilute, so that at very low temperatures only interactions between atoms of different species are allowed. The gas is described in terms of the one-body distribution functions $f^{(s)}(\mathbf{r}, \mathbf{p}, t)$ for each species s and the particle densities are obtained by performing an integration over momentum space,

$$n^{(s)}(\mathbf{r}, t) = \int \frac{d^3 \mathbf{p}}{(2\pi\hbar)^3} f^{(s)}(\mathbf{r}, \mathbf{p}, t). \quad (2)$$

The distribution functions at equilibrium are given by the local Fermi-Dirac distributions

$$f_0^{(s)}(\mathbf{r}, \mathbf{p}) = \left\{ \exp \left[\beta \left(\frac{p^2}{2m} + U^{(s)}(\mathbf{r}) - \mu^{(s)} \right) \right] + 1 \right\}^{-1}, \quad (3)$$

where $\beta = 1/k_B T$ with T the temperature, $\mu^{(s)}$ is the chemical potential ensuring the normalization $N_s = \int f^{(s)}(\mathbf{r}, \mathbf{p}) d^3 r d^3 p / h^3$, and the mean-field potentials read

$$U^{(s)}(\mathbf{r}) = V_{\text{ext}}(\mathbf{r}) + g n^{(\bar{s})}(\mathbf{r}). \quad (4)$$

Here \bar{s} denotes the component different from s and $g = 4\pi\hbar^2 a/m$ is the coupling strength between atoms of different species, with a being their s -wave scattering length.

The calculation of the equilibrium density profiles $n_0^{(s)}$ requires the self-consistent solution of equations (2)-(4) for each set of system parameters. At $T = 0$ the results

of the Thomas-Fermi approximation are recovered, giving $n_0^{(s)}$ as the solution of the equation $\mu(n_0^{(s)}) + V_{\text{ext}}(\mathbf{r}) = \mu^{(s)}$, with $\mu(n)$ the equation of state of the gas

$$\mu(n_0^{(s)}) = \frac{\hbar^2}{2m} \left(6\pi^2 n_0^{(s)} \right)^{2/3} + g n_0^{(\bar{s})}. \quad (5)$$

We shall study a mixture of 2000 ^{40}K atoms at $T = 0.2T_F$, T_F being the Fermi temperature. The atoms are equally distributed in two spin states and confined inside a trap with radial frequency $\omega_{\perp} = 100 \text{ s}^{-1}$. Hereafter we will remove the indices s and \bar{s} when there is no ambiguity and set $\mu^{(s)} = \mu^{(\bar{s})} = \mu$ and $n^{(s)} = n^{(\bar{s})} = n$.

2.1. Sound propagation

The time evolution of the one-body distributions strongly depends on the frequency of the inter-species collisions. When this is much lower than the trap frequency, the evolution of the gas is governed by deformations of the Fermi sphere and the dynamics is termed collisionless. This is the regime of zero sound. In a homogeneous mixture the collisionless sound velocity is given by $c_0 = \eta v_F$, with the Fermi velocity $v_F = [2(\mu - g n_0)/m]^{1/2}$. The ratio η can be calculated in Landau's Fermi-liquid theory describing the mean-field interactions through appropriate Landau parameters. For a two-component Fermi gas with negligible interactions between atoms of the same spin, η satisfies the relation [14, 17]

$$\frac{\eta}{2} \ln \frac{\eta + 1}{\eta - 1} - 1 = \frac{\pi \hbar}{2m v_F a}. \quad (6)$$

In a trap one may use a local-density approximation and assign the position-dependent Fermi velocity $v_F(\mathbf{r}) = [2(\mu - V_{\text{ext}}(\mathbf{r}) - g n_0(\mathbf{r}))/m]^{1/2}$ to the atoms, provided the variation of the density profile is sufficiently smooth. In this way the confinement is accounted for only through the position dependence of the density profiles.

However, a very tight confinement may drastically modify the density of states of the gas and thus the dynamic of density perturbations. The zero sound velocity \tilde{c}_0 in strongly elongated traps ($\lambda \rightarrow 0$ and $V_{\text{ext}}(\mathbf{r}) \rightarrow m\omega_{\perp}^2 r_{\perp}^2/2$), in a regime where the degrees of freedom in the azimuthal plane are frozen by the confinement, is given by (see Appendix)

$$\tilde{c}_0 = v_F^0 \left(1 + \frac{2\hbar a}{\pi \tilde{a}_{\perp}^2 m v_F^0} \right)^{1/2}, \quad (7)$$

with v_F^0 being the local Fermi velocity at the centre of the trap and $2\pi \tilde{a}_{\perp}^2$ the radial section of the atomic cloud. This velocity coincides with that of a strictly one-dimensional (1D) Fermi gas [18, 19] with an effective coupling $2\hbar^2 a / (m \tilde{a}_{\perp}^2)$ embodying the transverse confinement [20].

Interactions between the two components make the sound velocity deviate from v_F by only a few percent for couplings up to $a = 2 \times 10^4$ Bohr radii for both the homogeneous and the cigar-shaped gas [17]. The effects of the interactions have also been investigated in the random-phase approximation for a Fermi gas in a spherical trap

in the collisionless regime [21,22]. The main outcome is the appearance of a fragmented excitation spectrum at strong couplings and of Landau-damped modes for attractive interactions. However, the confinement introduces a discrete single-particle excitation spectrum that may weaken the strength of the damping. In a cigar-shaped confinement, the sound velocity given in equation (7) is well defined for repulsive interactions as well as sufficiently weak attractive interactions, analogously to zero sound in a 1D Fermi gas [19].

When the dynamics is instead governed by the hydrodynamic equations, the (first) sound velocity in a homogeneous gas is given by

$$c_1 = \frac{v_F}{\sqrt{3}} \left(1 + \frac{2a}{\pi} \frac{mv_F}{\hbar} \right)^{1/2}, \quad (8)$$

showing that the explicit dependence on the scattering length is qualitatively similar to that in equation (7). In addition to the density modes, an oscillation of the spin density $\xi = n^{(s)} - n^{(\bar{s})}$ may develop depending on how the gas is perturbed [23–25]. In fact, for strong repulsions the two species tend to segregate into two non-overlapping regions. For attractive interactions, the system will become unstable and experience a sudden collapse when the sound velocity vanishes. However, at very low temperatures the collapse may be prevented by a transition to a superfluid phase [2, 26, 27] or by pairing of the atoms into molecular dimers [28–30].

With the purpose of examining the confinement effects on the propagation of first sound, we consider again a radially confined Fermi gas and assume a density wave travelling in the axial z direction. In this case we have shown [11] that the first sound velocity \tilde{c}_1 depends on the equation of state through the relation

$$\tilde{c}_1 = \left(\frac{1}{m} \int n_0 d^2 r_\perp / \int (\partial\mu/\partial n|_{n_0})^{-1} d^2 r_\perp \right)^{1/2} \quad (9)$$

where the integration is on the azimuthal plane. Equation (9) reduces to equation (8) for a homogeneous Fermi gas and yields $\tilde{c}_1 = v_F^0/\sqrt{5}$ for the cigar-shaped Fermi gas without mean-field interactions. More generally, numerical integration can be carried out once the equilibrium density is known.

3. Density waves at finite collisionality

Neither the collisionless nor the hydrodynamic approach is appropriate when the number of collisions is sizable but not sufficient to establish local equilibrium in the gas. One must then resort to kinetic equations and can use a Boltzmann equation method to take into account binary collisions in a semiclassical manner. The evolution of the one-body distributions is determined by the VLE

$$\partial_t f^{(s)} + \frac{\mathbf{p}}{m} \cdot \nabla_{\mathbf{r}} f^{(s)} - \nabla_{\mathbf{r}} U^{(s)} \cdot \nabla_{\mathbf{p}} f^{(s)} = C^{(s)}[f^{(s)}, f^{(\bar{s})}], \quad (10)$$

where the collision integral $C^{(s)}$ reads

$$C^{(s)} = \frac{\sigma}{4\pi(2\pi\hbar)^3} \int d^3 p_2 d\Omega_f v [(1 - f^{(s)})(1 - f_2^{(\bar{s})})f_3^{(s)}f_4^{(\bar{s})}$$

$$-f^{(s)}f_2^{(\bar{s})}(1-f_3^{(s)})(1-f_4^{(\bar{s})})]. \quad (11)$$

Here $f^{(s)} \equiv f^{(s)}(\mathbf{r}, \mathbf{p}, t)$ and $f_i^{(s)} \equiv f^{(s)}(\mathbf{r}, \mathbf{p}_i, t)$, $d\Omega_f$ is the element of solid angle for the outgoing relative momentum $\mathbf{p}_3 - \mathbf{p}_4$, $\sigma = 4\pi a^2$ is the scattering cross-section, and $v = |\mathbf{v} - \mathbf{v}_2|$ is the relative velocity of the incoming particles. The collision satisfies conservation of momentum ($\mathbf{p} + \mathbf{p}_2 = \mathbf{p}_3 + \mathbf{p}_4$) and energy ($\varepsilon + \varepsilon_2 = \varepsilon_3 + \varepsilon_4$), with $\varepsilon_i = p_i^2/2m + U^{(s_i)}$.

The propagation of a density perturbation is evaluated by performing the following numerical experiment. First we construct the equilibrium density profiles according to equations (2)-(4) for a given confinement configuration and interaction strength. A Gaussian potential $U_0 \exp(-z^2/2w^2)$ with amplitude $U_0 = 10\hbar\omega_\perp$ and width $w = (\hbar/(m\omega_\perp))^{1/2}$ is then switched on at the centre of the trap to simulate a laser beam expelling particles from the centre of the cloud. At later times these density distortions are seen to move towards the ends of the trap. Since each perturbation has velocity mainly in the z direction, we focus on the evolution of the integrated density profile $\tilde{n}(z) = \int n(\mathbf{r}) d^2r_\perp$. Experimentally, this density can be obtained directly from *in-situ* measurements of the three-dimensional density profiles. In figure 1 we plot $\tilde{n}(z)$ at several times for a trap with $\lambda = 0.1$ and for three values of the scattering length, namely $a = -1.5 \times 10^4$, 80, and 2×10^4 Bohr radii a_0 . At larger attractions the gas collapses, whereas for larger repulsions the effects of demixing become noticeable. We follow the positions of the main density peaks created by the Gaussian potential and plot in figure 2 their evolution in time. After a hole in the density has been created, we observe that density pulses travel with constant speed in the neighbourhood of the trap centre. For $a = -1.5 \times 10^4 a_0$ and $2 \times 10^4 a_0$ it can be seen that the slope of the peak positions clearly departs from \tilde{c}_0 and moves closer to \tilde{c}_1 , as the hydrodynamic regime is being approached.

The results for the sound velocity as a function of the coupling are summarized in figure 3, where we show the mean value $\langle v_z \rangle = \frac{1}{2}(\langle v_z^{(s)} \rangle + \langle v_z^{(\bar{s})} \rangle)$ of the time-averaged velocities of the two components of the mixture as obtained from the solution of the VLE. These have been evaluated over a time interval $\Delta t = 1.5/\omega_\perp$ starting at $t_0 = 1/\omega_\perp$. In the same figure we also report the results of the analytical models introduced in Sec. 2.1, *i.e.* the zero-sound velocity \tilde{c}_0 in a strongly elongated trap (cf. equation (7)), and the first-sound velocity \tilde{c}_1 in a strongly elongated trap as given in equation (9) with $n^{(s)} = n^{(\bar{s})}$. In the latter case we have used the zero-temperature equation of state (5) and set μ to the value obtained in the VLE simulation. By solving the VLE in the absence of collisions we also find that the speed of the density perturbations is well defined for both positive and negative couplings and follows the trend of \tilde{c}_0 as a function of a (not shown in the figure). We emphasize that in the absence of collisions zero sound is a well defined collective excitation in the gas under quasi-1D confinement even when the interactions between the particles are attractive, contrary to the case of a homogeneous 3D gas where these excitations are stable only for interparticle repulsions [14]. On the other hand, in the case of repulsive interactions our results for \tilde{c}_0 are very close to those obtained from equation (6) for the homogeneous gas.

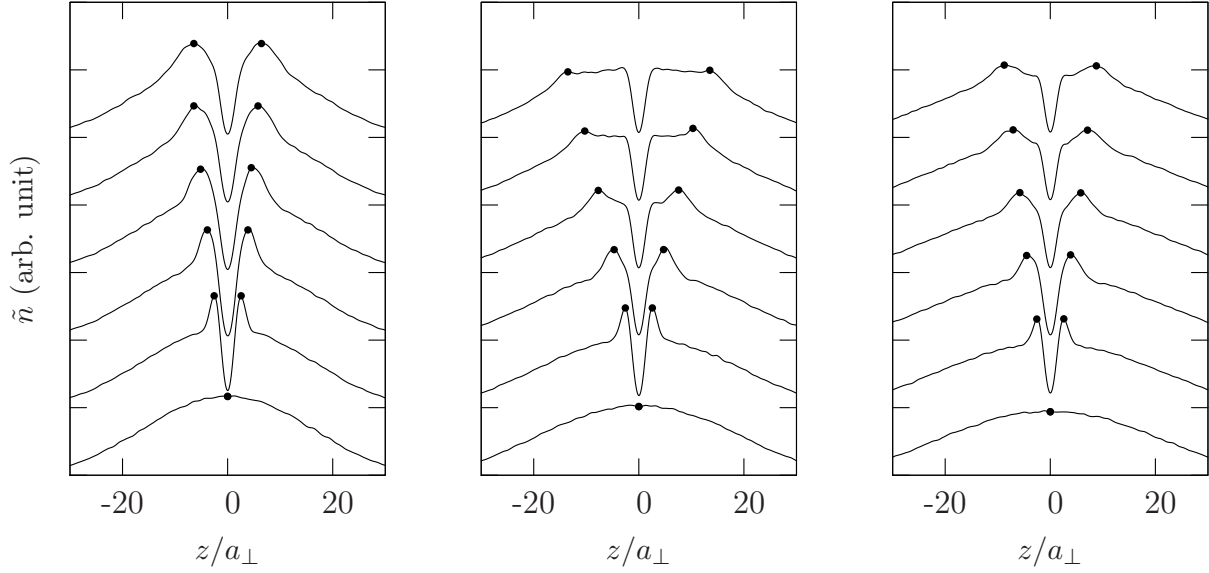


Figure 1. Time evolution of the integrated density profile $\tilde{n}(z)$ as a function of axial position z (in units of $a_{\perp} = \sqrt{\hbar/(m\omega_{\perp})}$) for 2000 ^{40}K atoms in a trap with $\lambda = 0.1$. The left, middle, and right panels correspond to $a = -1.5 \times 10^4, 80$, and 2×10^4 Bohr radii, respectively. The bottom profile refers to the initial equilibrium state and the subsequent ones are separated by time intervals of $0.5/\omega_{\perp} = 5$ ms. The later profiles have been vertically displaced for the sake of visibility.

From the full solution of the VLE including collisions, we observe that at low coupling the velocity of the density perturbations is close to \tilde{c}_0 within the error bars. In this regime the value of the sound velocity is dominated by the mean-field interactions and their effect on sound propagation can be understood as mainly resulting from changes in the local density: in particular, for attractive coupling the Fermi velocity and the sound velocity rise as the density of the gas is increased. At stronger coupling strength the sound velocity drops for both positive and negative coupling, as opposed to the behaviour of the collisionless velocity \tilde{c}_0 . This drop is more pronounced for attractive coupling as the frequency of collisions increases with $|a|$ as well as with the gas density, whereas at strongly repulsive interactions the collisions increase more slowly as the two components approach spatial demixing. This effect is not included in the calculation of \tilde{c}_1 . At strongly attractive interactions the frequency of collisions is much larger than ω_z and therefore the gas is strongly collisional. The difference between $\langle v_z \rangle$ and \tilde{c}_1 at $a = -1.5 \times 10^4 a_0$ may be attributed to the appreciable amplitude of the density perturbations as well as to the confinement in the axial direction. At strong coupling, although the rate of collisions in the axially confined inhomogeneous cloud varies at each point in space during the propagation of the pulse, the sound wave travels without observable damping in the neighbourhood of the trap centre.

The behaviour of $\langle v_z \rangle$ for two values of the anisotropy parameter at fixed ω_{\perp} is illustrated in figure 4. In the top panel we report the Fermi velocity at the cloud centre for both components, showing that in the more elongated cloud the density of the gas

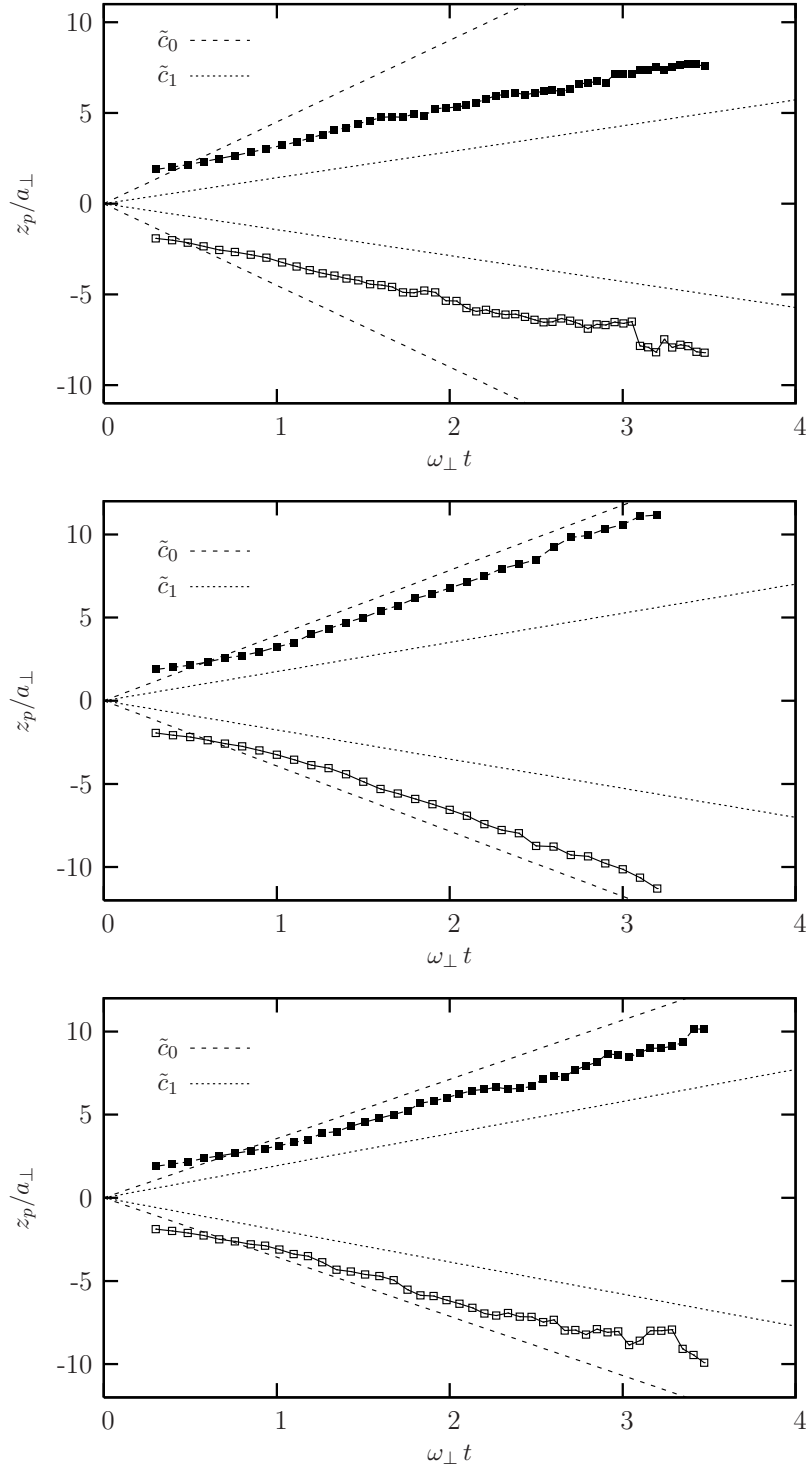


Figure 2. Location z_p/a_\perp of the density peaks in $\tilde{n}(z)$ as a function of time (in units of $1/\omega_\perp$). The top, middle, and bottom panels correspond to $a = -1.5 \times 10^4$, 80, and 2×10^4 Bohr radii. The dashed and dotted lines refer to propagation at the zero-sound velocity \tilde{c}_0 and at the first-sound velocity \tilde{c}_1 , respectively.

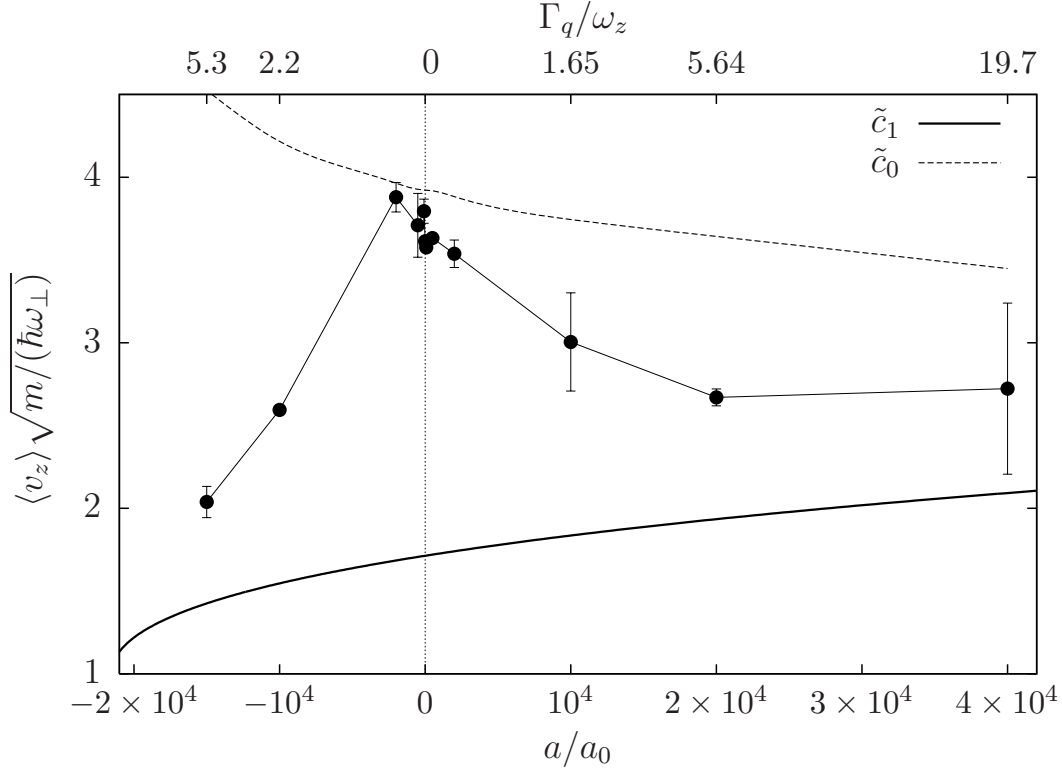


Figure 3. Average velocity $\langle v_z \rangle$ (in units of $\sqrt{\hbar\omega_\perp/m}$) as a function of the scattering length a (in units of the Bohr radius a_0) for $\lambda = 0.1$. The thick solid line and the dashed line show the sound velocity calculated in the absence of damping as for first sound and zero sound, respectively. The dots with error bars are the results of the VLE simulation, the errors being estimated from the noise in the slope of the density peak positions in figure 2. The thin solid line is just a guide to the eye. The scale at the top gives the quantum collision rate Γ_q (in units of ω_z).

and thus the Fermi velocity are lower. Therefore, at a fixed value of a the collisionality of the gas with $\lambda = 0.06$ is lower and $\langle v_z \rangle/v_F^0$ is higher (bottom panel of figure 4). On the other hand, if we fix the average trap frequency and thus the density at the centre, a deformation of the trap would increase the number of collisions occurring during sound propagation and therefore facilitate the transition towards the hydrodynamic limit [31]. The effect of demixing at strong repulsive interaction is also illustrated in the top panel of figure 4.

4. Summary and concluding remarks

We have studied the propagation of sound waves in a mixture of fermionic atoms confined inside a strongly elongated cigar-shaped trap and exposed to the role of collisions in determining the speed of propagation. We have compared our results from the numerical solution of the Vlasov-Landau equations with two limiting behaviours: zero sound and first sound propagating in an infinitely long cylindrical cloud with a very tight transverse confinement. We have found substantial agreement between the velocity of density

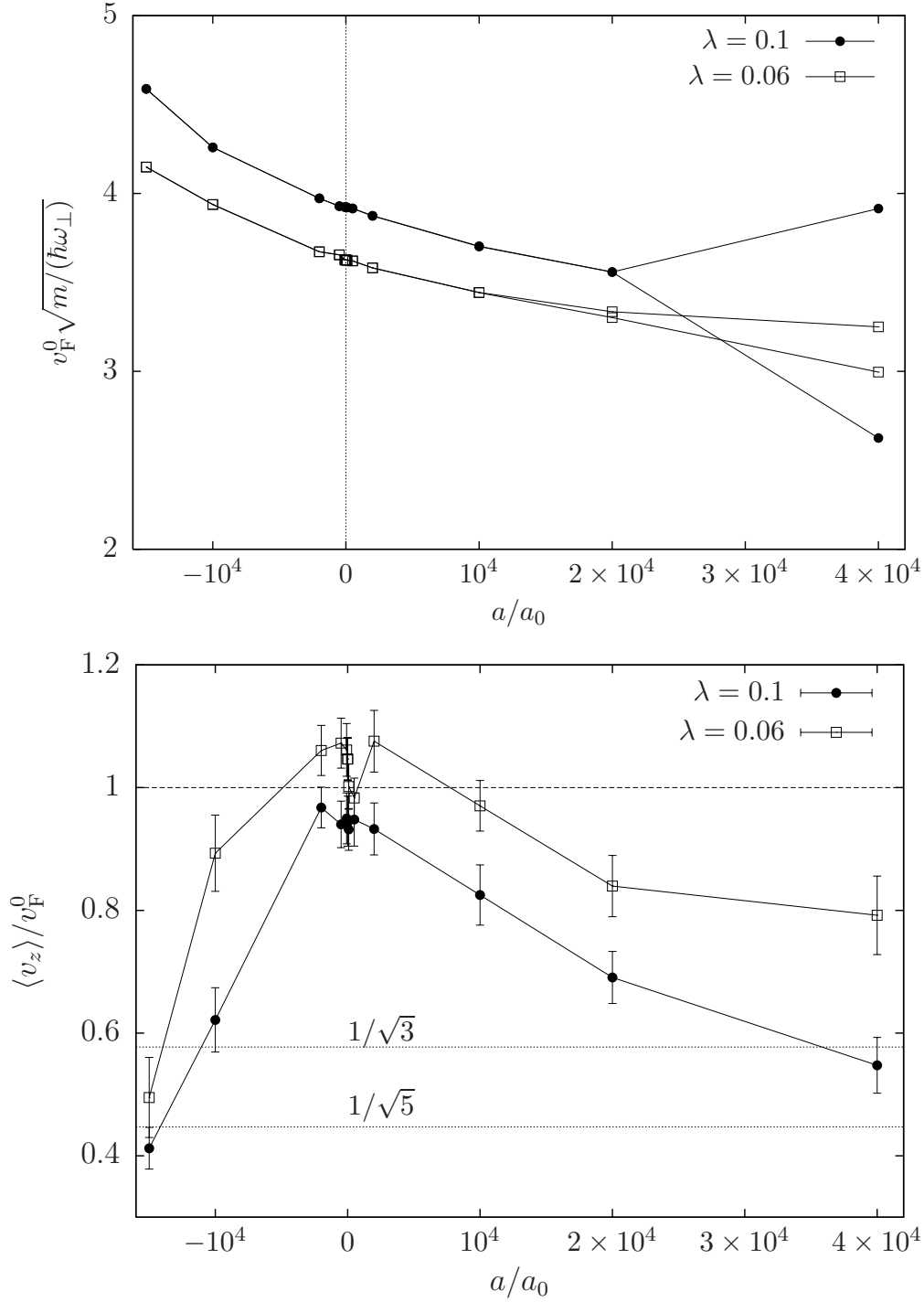


Figure 4. Sound velocity in elongated traps with $\lambda = 0.1$ or $\lambda = 0.06$. Top panel: Local Fermi velocity v_F^0 at the cloud centre (in units of $\sqrt{\hbar\omega_\perp/m}$) as a function of a (in units of the Bohr radius). Bottom panel: Average sound velocity (in units of v_F^0) as a function of a (in units of the Bohr radius).

perturbations in the collisionless regime and in the highly collisional regime with those of zero sound and first sound, respectively. The differences may be attributed to the finite amplitude of the density perturbations that we have produced and to the axial confinement.

It would be interesting to study the effect of the presence of a superfluid component on the zero-to-first sound transition at finite temperature. This can be done by using suitable transport equations for a trapped Fermi gas below the superfluid transition temperature, as already treated by Urban and Schuck [12].

Acknowledgments

This work has been partially supported by an Advanced Research Initiative of Scuola Normale Superiore di Pisa and by the Istituto Nazionale di Fisica della Materia within the Initiative “Calcolo Parallelo”.

Appendix A. Zero sound in a cylindrical trap

We apply the transport equation (10) with $C^{(s)} = 0$ and $V_{\text{ext}} = m\omega_{\perp}^2 r_{\perp}^2/2 \equiv \tilde{V}$ to evaluate the propagation of zero sound in a tight cylindrical trap. A density perturbation travels mainly along the axis of the cylinder when the radial confinement is strong, and the distribution function can be written as

$$f^{(s)}(\mathbf{r}, \mathbf{p}) = f_0^{(s)}(\mathbf{r}_{\perp}, \mathbf{p}) + f_1^{(s)}(\mathbf{r}_{\perp}, \mathbf{p})e^{i(kz - \omega t)} \quad (\text{A.1})$$

where $f_0^{(s)} = \theta(\mu^{(s)} - \frac{p_z^2}{2m} - \tilde{V}(r_{\perp}) - gn_0^{(\bar{s})}(r_{\perp}))$ is the equilibrium distribution. Around the centre of the azimuthal plane one can write $f_0^{(s)} = \theta(\tilde{\mu}^{(s)} - \frac{p_z^2}{2m} - \frac{p_{\perp}^2}{2m} - \frac{1}{2}m\tilde{\omega}_{\perp}^2 r_{\perp}^2)$ with $\tilde{\mu}^{(s)} = \mu^{(s)} - gn_0^{(\bar{s})}(0)$ and $\tilde{\omega}_{\perp} = \omega_{\perp}(1 - 3gn_0^{(\bar{s})}(0)/(2\mu))^{1/2}$. Only the first level in the radial harmonic potential with frequency $\tilde{\omega}_{\perp}$ is occupied by the fermions in a very tight radial confinement, and the distribution function takes the simple form $f_0^{(s)} = \theta(\tilde{\mu}^{(s)} - \frac{p_z^2}{2m} - \hbar\tilde{\omega}_{\perp})$.

The terms in the transport equation involving the derivatives with respect to r_{\perp} and p_{\perp} disappear if $f_1^{(s)}$ is a function of the total energy analogously to $f_0^{(s)}$. Equation (10) then becomes

$$\left(\frac{k p_z}{m} - \omega\right) f_1^{(s)} - \frac{k p_z}{m} \frac{\partial f_0^{(s)}}{\partial \varepsilon} \int \frac{d\mathbf{p}}{(2\pi\hbar)^3} g f_1^{(\bar{s})} = 0, \quad (\text{A.2})$$

where we have set $\varepsilon = p_z^2/(2m)$. The form of equation (A.2) suggests to write $f_1^{(s)}$ as proportional to $\nu \partial f_0^{(s)}/\partial \varepsilon$, ν being defined as

$$\nu = \begin{cases} \frac{1}{1 - \eta} & \text{if } k p_z > 0 \\ \frac{1}{1 + \eta} & \text{if } k p_z < 0 \end{cases} \quad (\text{A.3})$$

with $\eta = \omega/(kv_F^{(s)})$ and $v_F^{(s)} = \sqrt{2(\tilde{\mu}^{(s)} - \hbar\tilde{\omega}_\perp)/m}$. Thus equation (A.2) can be rewritten as

$$1 + \frac{g}{1 - \eta^2} \int \frac{d^3p}{(2\pi\hbar)^3} \delta(\tilde{\mu}^{(\bar{s})} - \frac{p_z^2}{2m} - \hbar\tilde{\omega}_\perp) = 0. \quad (\text{A.4})$$

Finally, we obtain

$$\eta = \sqrt{1 + \frac{2\hbar a}{\pi \tilde{a}_\perp^2 m v_F^{(\bar{s})}}}. \quad (\text{A.5})$$

by integrating over all p_z and $p_\perp \in [0, \sqrt{2\hbar m \tilde{\omega}_\perp}]$. This is equation (7) in the main text.

References

- [1] Gensemer S D and Jin D S 2001 *Phys. Rev. Lett.* **87** 173201
- [2] Kinast J, Hemmer S L, Gehm M E, Turlapov A and Thomas J E 2004 *Phys. Rev. Lett.* **92** 150402
- [3] Bartenstein M, Altmeyer A, Riedl S, Jochim S, Chin C, Denschlag J H and Grimm R 2004 *Phys. Rev. Lett.* **92** 203201
- [4] DeMarco B and Jin D S 2002 *Phys. Rev. Lett.* **88** 040405
- [5] Loftus T, Regal C A, Ticknor C, Bohn J L and Jin D S 2002 *Phys. Rev. Lett.* **88** 173201
- [6] Regal C A and Jin D S 2003 *Phys. Rev. Lett.* **90** 230404
- [7] Toschi F, Vignolo P, Succi S and Tosi M P 2003 *Phys. Rev. A* **67** 041605
- [8] Toschi F, Capuzzi P, Succi S, Vignolo P and Tosi M P 2004 *J. Phys. B* **37** S91
- [9] Ho T L 2004 *Phys. Rev. Lett.* **92** 090402
- [10] Heiselberg H 2005. *Preprint* cond-mat/0503101
- [11] Capuzzi P, Vignolo P, Federici F and Tosi M P 2005. *Preprint* cond-mat/0509323
- [12] Urban M and Schuck P 2005. *Preprint* cond-mat/0509373
- [13] Heiselberg H 2004. *Preprint* cond-mat/0409077
- [14] See *e.g.* Pines D and Nozières P 1994 *The Theory of Quantum Liquids* Vol. 1 (New York: Addison-Wesley)
- [15] Abel W R, Anderson A C and Wheatley J C 1966 *Phys. Rev. Lett.* **17** 74
- [16] Andrews M R, Kurn D M, Miesner H J, Durfee D S, Townsend C G, Inouye S and Ketterle W 1997 *Phys. Rev. Lett.* **79** 553
- [17] Akdeniz Z, Vignolo P and Tosi M P 2003 *Phys. Lett. A* **311** 246
- [18] Apostol M and Malomed B A 1992 *Phys. Rev. B* **45** 4509
- [19] Hernández E S 2002 *J. Low Temp. Phys.* **127** 153
- [20] Salasnich L, Parola A and Reatto L 2002 *Phys. Rev. A* **65** 043614
- [21] Capuzzi P and Hernández E S 2001 *Phys. Rev. A* **63** 063606
- [22] Bruun G M 2001 *Phys. Rev. A* **63** 043408
- [23] Vichi L and Stringari S 1999 *Phys. Rev. A* **60** 4734
- [24] Bruun G M and Clark C W 1999 *Phys. Rev. Lett.* **83** 5415
- [25] Amoroso M, Meccoli I, Minguzzi A and Tosi M P 2000 *Eur. Phys. J. D* **8** 361
- [26] Chin C, Bartenstein M, Altmeyer A, Riedl S, Jochim S, Hecker Denschlag J and Grimm R 2004 *Science* **305** 1128
- [27] Zwierlein M W, Abo-Shaeer J R, Schirotzek A, Schunck C H and Ketterle W 2005 *Nature* **435** 1047
- [28] Greiner M, Regal C A and Jin D S 2003 *Nature* **426** 537
- [29] Jochim S, Bartenstein M, Altmeyer A, Hendl G, Riedl S, Chin C, Denschlag J H and Grimm R 2003 *Science* **302** 2101
- [30] Zwierlein M W, Stan C A, Schunck C H, Raupach S M F, Gupta S, Hadzibabic Z and Ketterle W 2003 *Phys. Rev. Lett.* **91** 250401
- [31] Capuzzi P, Vignolo P and Tosi M P 2005 *Phys. Rev. A* **72** 013618